The stability of collinear bundles and the influence of a time-periodic load on the forward propulsion of spermatozoa

M.W.Hoppenreijs

University of Twente, Faculty of Engineering Technology - Biomechanical Engineering, Drienerlolaan 5, 7522 NB, Enschede, The Netherlands
m.w.hoppenreijs@student.utwente.nl

ABSTRACT: Minimally invasive medicine is an uprising technology. Soft microrobots are used in invasive medicine to transport drugs to target cells. The analogy between soft microrobots and sperm cells can be made due to their structure and their purpose. Sperm cells have a wide variety in number of flagella and the configuration of their flagella with respect to each other. Detailed videos of sperm cells show these different sperm cells and can be observed. From these videos data can be obtained using Matlab. The wave variables that describe the wave of the flagellum, the thrust force induced by a tail and the flowfield around a tail can be mapped. An interesting case is a collinear bundle which has 2 flagella around 1 head, where both flagella are 180° away from each other. This paper shows how this bundle is stable and remains at its 180° configuration, where usually 2 flagellum would polarize to one side until the angle between them is 0°. The effect of steric and adhesive forces on the stability around 180° A flow field is made, comparing the collinear bundle, which can be seen as a time-periodic load, to a static-loaded case and a free swimming cell.

Key words: Minimally invasive medicine, Soft microrobots, spermatozoa, collinear bundle, steric forces, adhesive forces time-periodic load, static load, free swimming cell, Resistive force theory, Regularized stokeslets, wave variables of collinear bundle

1 INTRODUCTION

In healthcare, minimally invasive medicine is an uprising technology. Reason for this is that minimally invasive medicine has multiple advantages over invasive medicine. Surgical operations that make use of invasive technology and involve great risks due to human errors may be replaced for minimally invasive medicine, as it reduces the risks harshly. Also, some surgical operations may become less expensive when minimally invasive medicine is used as a treatment. Lastly, some areas within the human body are difficult to access using tethered robotic systems or invasive medicine which leaves incurable parts in the human body that can be cured with minimally invasive medicine [1]. Now that the advantages of minimally invasive medicine are mentioned, a short introduction to this subject should be described.

Minimally invasive medicine technology makes use of soft microrobots which are able to develop themselves through a medium of bodily fluids. The main goal of using soft microrobots is to use them as a mean to propagate the drug necessary to cure a certain cell within the body of an organism. The cell that needs curing is often referred to as a so called ”target cell” and in order to cure this cell a drug is used. A soft microrobot exists of roughly 2 main structures, one structure being one or multiple tails and the other structure being the head of the microrobot (figure 1). The head is oftenly used as a storage part of the microrobot for the drug necessary to cure the target cell. When a soft microrobot arrives at the target cell the drug can be released and the target cell may be cured. The tail like structures are referred to as flagella. These flagella make move in a sine-wave configuration, generating thrust force for the soft microrobot. This way, the microrobot is able to propagate itself forward in a medium of bodily fluids. The thrust force generated by the flagella overcomes the problem that Reynolds numbers, in human bodily fluids, are often very low [2]. This results in difficulties regarding propulsion but are solved by using flagella that are controlled with a micro motor.

Since the structure of soft microrobots comes very close to that of spermatozoa, an analogy can be made between the two. Experimenting with microrobots can become expensive but because of the close analogy experiments can be done with spermatozoa instead. Doing this and observing the behaviour of different spermatozoa in different environments and modelling them gives valuable insights for the technology of soft microrobots.

Due to high propulsion power requirements it is important that experiments are performed from which it becomes clear what spermatozoa structures are the most efficient swimmers. Different structures include the number of flagella one sperm cell its head has and the configuration of the flagella with respect to each other. An interesting case is when two flagella form a collinear bundle, in which the angle between both tails is equal to $180°$. An interesting property of the collinear bundle is that they can switch direction of propulsion without making a wide U-turn, unlike polarized bundles [3]. This property can be very useful when a soft microrobot has to propegate itself forward and backwards in a very narrow vein, in which larger U-turns are not possible.

Collinear bundles can be modelled as a sperm cell that undergoes a time periodic load from the second tail. In this thesis, the formation and stability of collinear bundles is discussed. Furthermore it is shown how wave variables can be obtained which describe the behaviour of the collinear bundle in the fluid. Lastly, Resistive Force Theory (RFT) and Regularized Stokeslets Theory (RST) can be used to find the forces acting on the collinear bundle and the flow-field of the surrounding fluid around the collinear bundle respectively.

2 TRANSITION AND STABILITY OF COLLINEAR SPERM CELLS

Collision of sperm cells may form bundles consisting of one or more sperm cells [4]. When collisions happen, the bundling consists of roughly three phases and during these phases the waveform can vary [5].

The first phase is the far field-to-locking phase, in this phase 2 sperm cells are subjected to a far field flow created by surrounding sperm cells. After this, the sperm cells may lock on to each other forming one sperm cell with two tails of which the angle difference between the two tails can be described as $\delta\Theta(^\circ)$.

The second phase is the spin rolling phase during which the sperm cells undergoes spinning movement where the angle between both tails is adjusted until the sperm cell is in a stable configuration. Previous research has shown that for most sperm cells that form a bundle, the angle difference between the two flagella $\delta\Theta(^\circ) = 0$ is stable.

The last phase is the steady swimming phase wherein the sperm cell travels forward with a constant wave-

Fig. 1: Free swimming sperm cell with one flagellum.

form. In order to describe the behaviour that $\delta\Theta$ converges to zero over time, a closer look has to be taken at the moment equations governing the transition. First, the total moments of each sperm cell during the spin-rolling transition phase can be written as:

$$ {}^1\mathbf{M}(t) = {}^1\mathbf{M}_{\text{head}}(t) + \kappa\left(\Theta_1(t) - \Theta_2(t)\right) + \int_0^{L_1} \mathbf{r}_1(s,t) \times \mathbf{f}_1(s,t)\mathrm{d}s = 0, \quad (1) $$

$$ {}^2\mathbf{M}(t) = {}^2\mathbf{M}_{\text{head}}(t) - \kappa\left(\Theta_1(t) - \Theta_2(t)\right) + \int_0^{L_2} \mathbf{r}_2(s,t) \times \mathbf{f}_2(s,t)\mathrm{d}s = 0, \quad (2) $$

From the equations it can be seen that the total moment consists of the hydrodynamic torque on the head of the sperm cells ${}^1\mathbf{M}(t)$, ${}^2\mathbf{M}(t)$ and an integral, which describes the moments from the tail of the sperm cell.

Combining both expressions and using linearity of the drag torque gives the following inhomogeneous first order differential equation:

$$ 8\pi\eta ab^2 C\left(\Omega_1 - \Omega_2\right) + 2\kappa\left(\Theta_1 - \Theta_2\right) + {}^1\mathbf{M}_{\text{flag}} - {}^2\mathbf{M}_{\text{flag}} = 0, \quad (3) $$

for this one unique solution exists for formula 3:

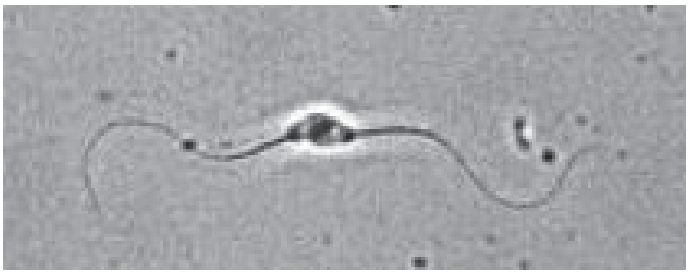

Fig. 2: Frame of a video containing a collinear bundle. It can be seen that the angle between both tails is equal to $\delta\Theta(^\circ) = 180$.

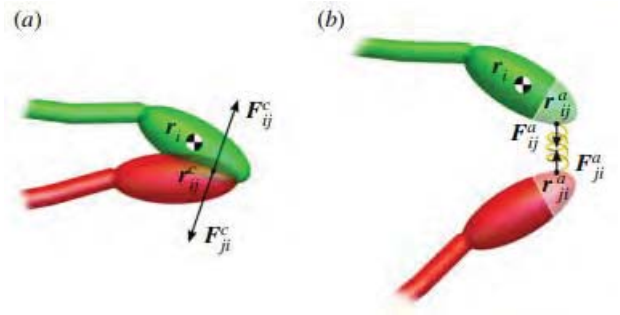

Fig. 3: a) Steric forces push the other sperm cell its head away, b) Adhesive forces can be modelled as a linear spring force which exists when the adhesive regions of both spermcells are within distance l_a [6].

$$\Delta\Theta(t) = \left(\frac{1}{8\pi\eta a b^2 C}\int_0^t \left({}^1\mathbf{M}_{\text{flag}} - {}^2\mathbf{M}_{\text{flag}}\right)\mathrm{d}t - \Delta\Theta_0\right) * \exp\left(\frac{-2\kappa}{8\pi\eta a b^2 C}t\right). \quad (4)$$

In order to explain collinear behaviour, it needs to be described how experimental results in which collinear bundles are formed $\delta\Theta(^\circ) = 180$ can stay in a collinear configuration rather than converging to $\delta\Theta(^\circ) = 0$. A collinear bundle is displayed in figure 2

An approximation can be made in which formula 4 can be rewritten for small and large initial angles $\Delta\Theta_0$. Formation of a collinear bundle exists for large initial angles $\Delta\Theta_0$ for which a formula for the first derivative of $\Delta\Theta(t) = \alpha$ can be rewritten as:

$$\dot{\alpha} = -\frac{2\kappa\sin\alpha + M_{\text{tail}}}{m}, \quad (5)$$

In this formula κ, is an interesting property which determines the final configuration of both tails with respect to the sperm cell its head. the variable κ can be dissected in two different constants with different signs [6] and are displayed in figure 3:

$$\kappa = \kappa_c - \kappa_a. \quad (6)$$

In this formula κ_c is an elastic constant which induces the steric interactions between two sperm cells (figure 3). The steric force resulting from this constant leads to the heads applying force away from the other sperm head leading to both tails being pushed away from one another. Secondly κ_a is the second elastic constant, which accounts for the adhesion between 2 sperm cells. It is modelled by a spring-like adhesion molecule. The molecules on the heads of the sperm cells causing this adhesion are localized to specific regions on the head of the sperm cells and an interactive force between 2 sperm heads may exist if the distance between the adhesive molecules is equal to or less than l_a. A so called Hookean spring is formed between the molecules of both heads and this tether remains while the absolute distance between both molecules is less than the interaction distance $|r^a_{ij} - r^a_{ji}| > l_a$. High adhesive forces induced by a high adhesive constant κ_a leads to the sperm heads remaining attached to each other, even though high steric forces are pushing both tails to a different side. This leads to a collinear bundle behaviour which can swim through a medium of viscous fluids. This observation of κ, can be introduced in the formula of of $\dot{\alpha}$, such that formula 5 can be rewritten to:

$$\dot{\alpha} = -\frac{2(\kappa_c - \kappa_a)\sin\alpha + M_{\text{tail}}}{m}, \quad (7)$$

Now the formula for $\alpha(t + \Delta t)$ can be constructed:

$$\alpha(t + \Delta t) = \alpha(t) + \dot{\alpha}\Delta t. \quad (8)$$

Using this formula in Matlab, a graph can be made which describes the progession of the angle difference, between collided sperm cells containing two flagella, $\Delta\Theta(t)$ in time dependent on the values of κ_a and κ_c.

From experiments, it is known that collinear behaviour is rather rare, meaning that the torque forces induced by the steric interaction forces often exceeds the adhesive forces which result from the adhesive

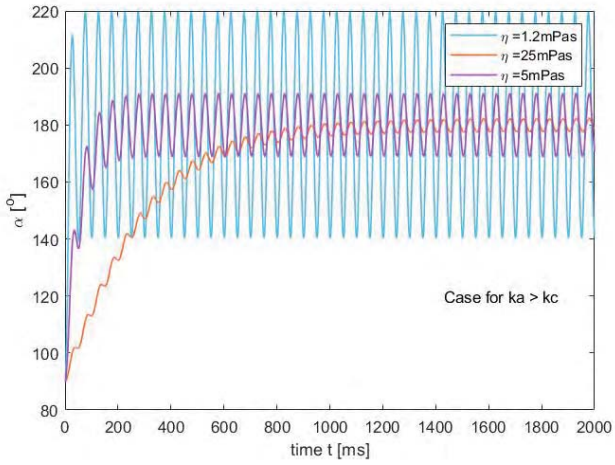

Fig. 4: collinear case in which $\kappa_a > \kappa_c$.

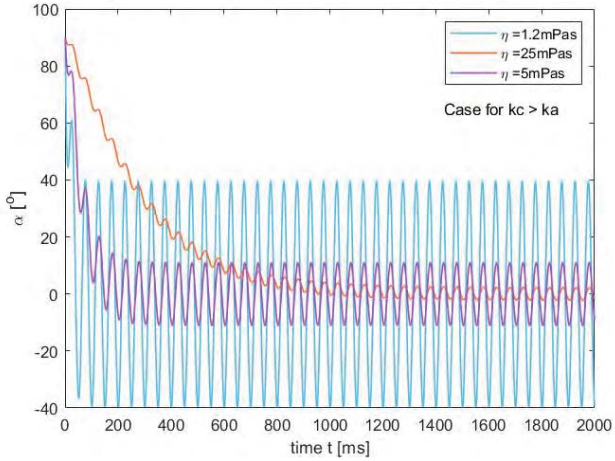

Fig. 5: Polarized case in which $\kappa_c > \kappa_a$.

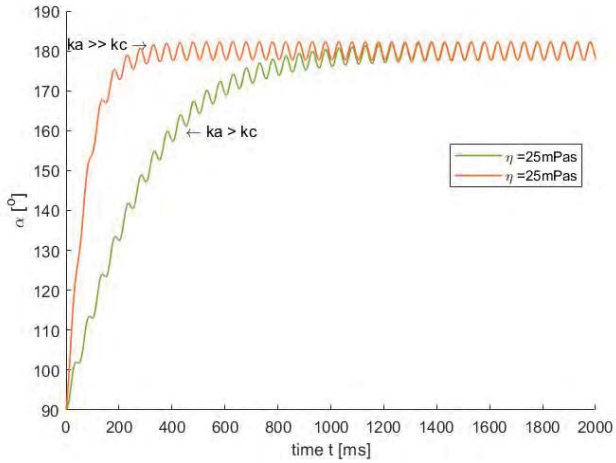

Fig. 6: Collision in medium with equal viscosity where the green line represents the case in which $\kappa_a > \kappa_c$ and the orange line represents the case $\kappa_a >> \kappa_c$.

constant κ_a. Therefore collinear cases are less common than polarized cases.

3 CHARACTERISTICS AND WAVE VARIABLES OF THE FLAGELLAR BEAT CYCLE

In order to approximate the configuration of a flagellum over one or more beat cycles, three wave variables can be used:

- A_0, the amplitude
- K_0, a measure for the assymetry, which the mean shape of the flagellum has
- λ, the wavelength

In order to obtain these variables, the zeroth and first Fourier mode are used which expresses the flagellar beat [7]. The Fourier series used can be described as:

$$\psi(s,t) \approx \tilde{\psi}_0(s) + \tilde{\psi}_1(s)e^{i\omega t} + \tilde{\psi}_1^* e^{i\omega t}, \tag{9}$$

Since the zeroth and first Fourier mode contribute to almost 95 $\%$ of the beat power, this formula well describes the flagellar beat.

Experiments have shown (ref friedrich) that each each term in equation 9 can be connected to the variables A_0, K_0 and λ. For this the line $K_0 s$ can be fitted to the zeroth mode $\tilde{\psi}_0(s)$, the line $A_0 s$ can be fitted to

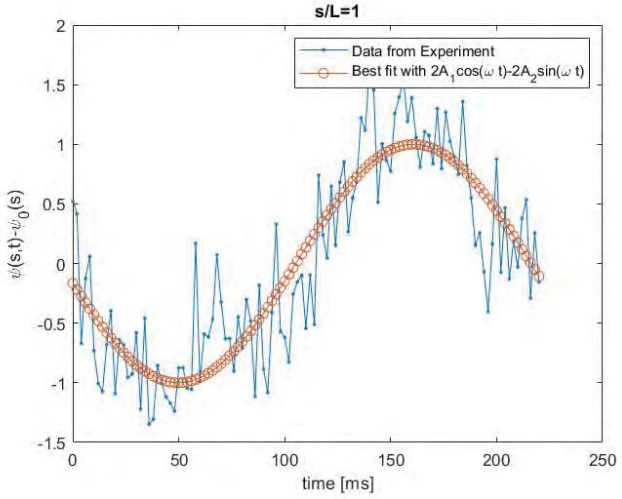

Fig. 7: sine approximation of the data

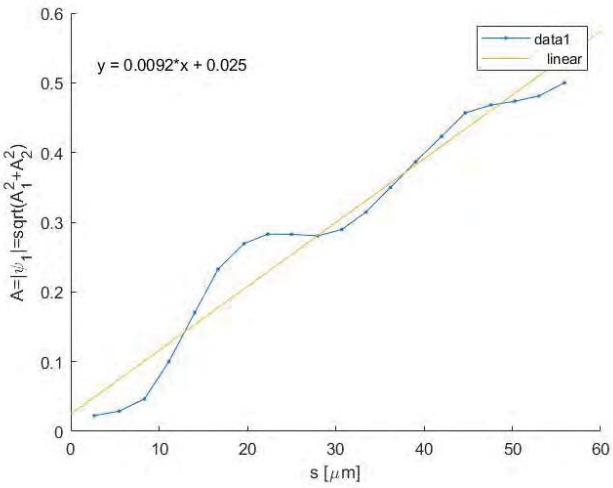

Fig. 8: graph to determine A_0

the first mode $|\tilde{\psi}_1(s)|$ and lastly the line $2\pi s/\lambda$ can be fitted to the last parameter in the equation $\phi(s) = -arg(\tilde{\psi}_1(s))$ which is the phase angle of the complex first mode. Combining this leads to equation 10.

$$\psi(s,t) = K_0 s + 2A_0 s\cos(\omega t - \frac{2\pi s}{\lambda}). \tag{10}$$

Matlab is able to use fourier to reconstruct the beat pattern. For this, a video of a real sperm sample needs to be split up in frames. In each frame the tail should be marked and these marked frames can then be used as an input for the matlab script (based on friedrich).

Because the beat pattern can be approximated as a sine wave, the reconstructed beat pattern by matlab should match a sine wave in order to confirm that the data is correct. This is shown in figure 7
After this check, the slopes of the three graphs containing either A_0,K_0 or ϕ (figure 8, 9 and 10 give the values of the wave variables A_0,K_0 and $2\pi/\phi$, respectively. These wave variables describe the given input beat pattern and can be calculated for each individual beat cycle.

When looking at collinear sperm cells, identifying beat cycles is difficult. For free swimming sperm cells the head of the sperm cell oscillates constantly and these oscillations are unhindered. However, collinear sperm bundles do not exhibit this behaviour. Since both tails try to swim, the combined sperm cell its head is unable to oscillate according to the swim

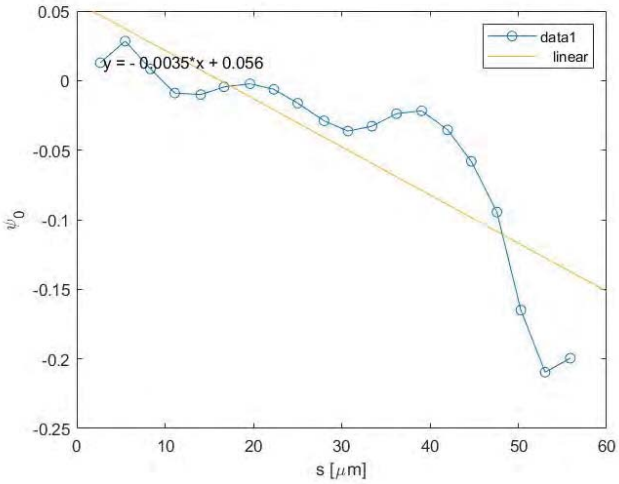

Fig. 9: graph to determine K_0

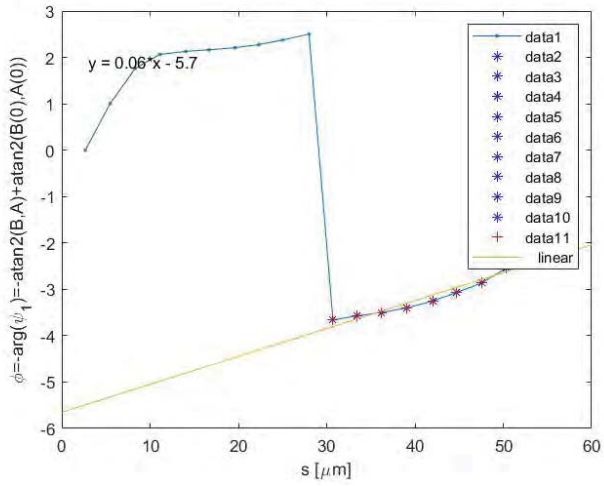

Fig. 10: graph to determine $\lambda = 2\pi/\phi$

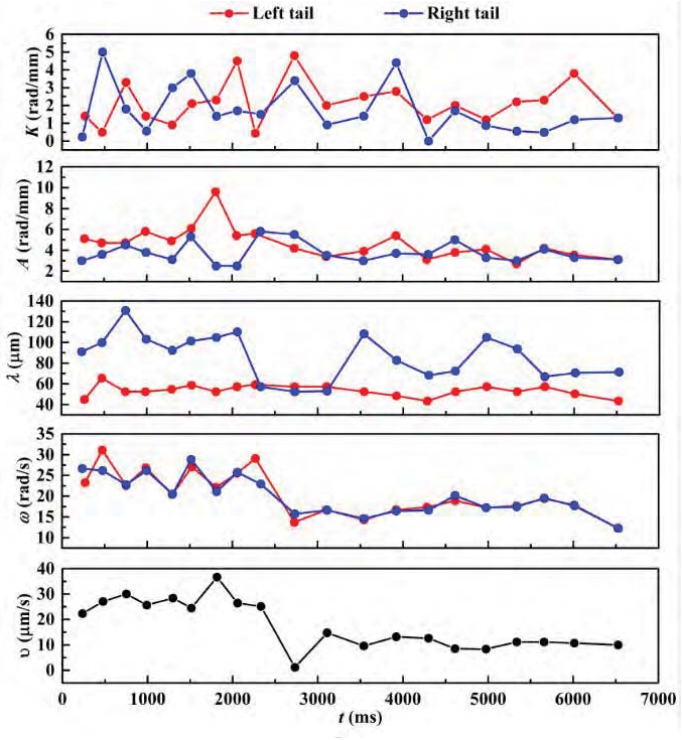

Fig. 11: Change of wave variables over time

pattern as it usually does. This leads to disturbances in the oscillation of the head as well as disturbances in the movement of the tail. Therefore the tail its beat pattern oftenly is not equal to a sine wave, but a disturbed sine wave. Because of this it is difficult to identify individual beat cycles and extract the correct wave variables that comply with each beat pattern.

Nevertheless, though these errors occur, the wave variables can be extracted for multiple consequent beat cycles and placed into a table. After this they can be placed in a graph which describes the change of each individual wave variable over time. If this graph starts the moment in time two sperm cells collide and form a collinear bundle, the three transition phases can be identified in the graph if the time interval also contains the steady swimming phase as described in section 2.

Because the formation of a collinear bundle is a rare process not many samples are available for research. The sample used only contained frames of the collinear bundle being in its steady swimming state. The graph with the changing wave variables is depicted in figure 11

The graph shows that the value of K_0 varies a lot over time. Since the value of K_0 is a measure for the assymetry it gives a good overview of how symmetric the tail moves over time in the sample. Single flagellar free swimming cells do not show this behaviour and have a value of K_0 which is far more constant during its steady swimming state. The results for the heavily fluctuating K_0 for collinear cells can be explained by the disturbed oscillations of the head. When one tail has a large positive value for K_0 it is relatively assymetric towards one side of the head in a 2-dimensional surface. However, when the second tail causes the head to move in the direction of the assymetry, the assymetry heavily decreases leading to large fluctuations that are not dependent on the movement of the first tail.

Secondly, it shows that the velocity $v(\mu m/s$ decreases at roughly $t = 2400ms$. When looking at the graphs above it can be observed that this is caused by the sudden decrease of the wavelength λ of the right tail at the same time instance. During the interval in which the velocity is low, the wavelength of both tails is equal. Because of this and the angular velocity ω, the thrust force of each tail is roughly the same. Since the thrust force of each tail works in opposite direction, the velocity of the collinear bundle decreases harshly.

4 RESISTIVE FORCE THEORY ON COLLINEAR SPERM CELLS

When looking at sperm cells, the movement of the sperm cells through a medium with a certain viscosity can be described by the bending waves in terms of the form and speed of propegation which travel along the tail. With this, also the forces that are exerted on the tail can be calculated.

Propulsive components of the forces acting normally to the surface of the sperm cell its body compensate the tangential forces acting along the sperm cell its body. Resistive force theory (RFT) [8] takes these forces into account and divides the tail of the sperm cell into small segments. In RFT the thrust force is related to coefficients of resistance to the surface of the segments for a medium with certain viscosity (C_N and C_L) and the tangential and normal displacements.

The thrust force of one small segment is described by the following formula:

$$dF = \left\{ \frac{(C_N - C_L)\frac{dy}{dt}\frac{dy}{dx} - V_x[C_L + C_N(\frac{dy}{dx})^2]}{1 + (\frac{dy}{dx})^2} \right\} ds, \quad (10.1)$$

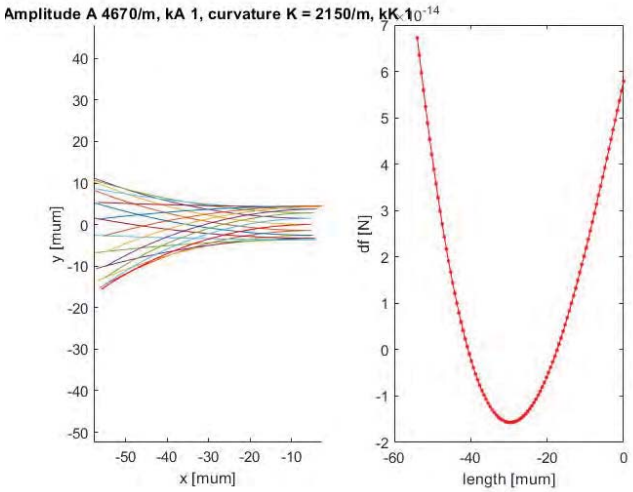

Fig. 12: Representation of the average bundle of the left tail in the collinear bundle and the thrustforce over the length of the tail

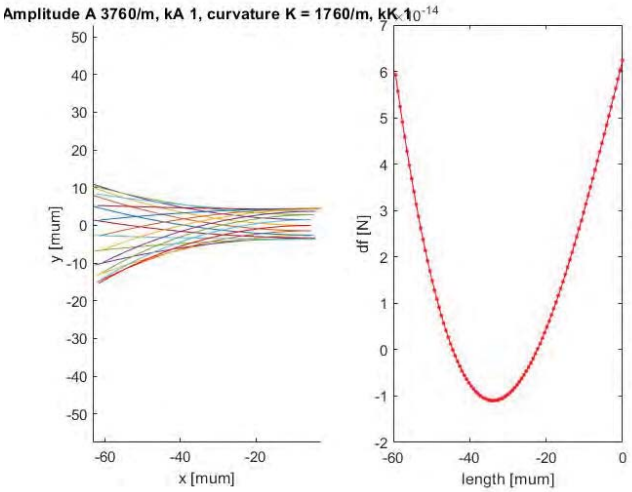

Fig. 13: Representation of the average bundle of the right tail in the collinear bundle and the thrustforce over the length of the tail. The sperm head is on the right side of the left figure. In reality the left picture should be rotated around the y-axis as the right tail has the head on the left side in the sample.

The above formula can be integrated. This way the force of all the segments can be calculated when integrating on an interval from 0 to λ. This gives the total force of the flagellum over one wave length:

$$F = \int_0^{\lambda} dF. \tag{11}$$

Matlab can make use of the above equations and is able to plot dF over time, as well as the form of the bundle. For this constants, such as the viscosity and the tail length, combined with the wave variables K_0, A_0 and λ are used as input values. Also the total force is calculated which is displayed in table 4. From the values obtained by Matlab it can be concluded that the average thrustforce of the left tail is stronger than the right tail, leading to the collinear bundle moving in the swimming direction of the left tail (to the right).

Tail:	Force (N)
Left Tail (1):	8.527×10^{-11}
Right Tail (2):	- $8{,}261\times10^{-11}$

Using the averaged wave variables in table 5.3, Matlab can model the average bundle of each tail and a graph of the thrust force at each segment dF over the length of the tail.

5 REGULARIZED STOKESLETS THEORY ON COLLINEAR SPERM CELLS

Using the theory of regularized stokeslets [9][10], a flowfield for the velocity of the fluid around the sperm cell can be obtained. This flow field gives valuable information about the flagellar propulsion of a sperm cell. Furthermore comparing cases between a free swimming one-tailed sperm cell, a fixed sperm cell (static loading with one constraint) and a sperm cell that undergoes a time periodic load is a good way to find out how the flow field of the medium around a sperm cell is influenced by a time periodic load.

The fluid response in RST can be described as:

$$\mathbf{u}(\mathbf{x}) = \sum_{i=1}^{M}\sum_{k=1}^{N} \frac{-{}^{i}\mathbf{F}_k}{4\pi\eta}\left[\ln\left(\sqrt{r_k^2+\epsilon^2}+\epsilon\right) - P\epsilon\right] + \frac{1}{4\pi\eta}\left[{}^{i}\mathbf{F}_k\cdot\left(\mathbf{x}-{}^{i}\mathbf{r}_k\right)\right]\left(\mathbf{x}-{}^{i}\mathbf{r}_k\right)P. \tag{12}$$

Where P is equal to:

$$P = \left[\frac{\sqrt{r_k^2+\epsilon^2}+2\epsilon}{\left(\sqrt{r_k^2+\epsilon^2}+\epsilon\right)^2\sqrt{r_k^2+\epsilon^2}}\right]. \tag{13}$$

In this formula $u(x)$ is the fluid response around the i^{th} filament and $r_k = |\mathbf{x} - {}^i\mathbf{r}_k|$ is the distance between the observation and the source point. The kinematics of the i^{th} filament can be described as a function of the tangent angle, leading to the following formula:

$$ {}^i\mathbf{r}(s,t) = {}^i\mathbf{r}(t) - a^i\mathbf{e}_1(t) - \int_0^s \cos^i \psi(v,t)^i\mathbf{e}_1(t) + \sin^i \psi(v,t)^i\mathbf{e}_2(t)\mathrm{d}v \quad (14) $$

In this formula ${}^i\mathbf{r}(t)$ is the position vector of the center of the sperm cell its head and $\psi_i(s,t)$ is the tangent angle which is also described in section 3, equation 10

Using Matlab, and the equations above the flow field of the fluid around one or multiple flagellum can be visualized in the form of graph. In order to do this Matlab takes wave variables as input values to simulate different flagella forms. Doing this, a collinear bundle case can be compared to a free swimming cell and a fixed cell in order to get a better understanding of a collinear bundle.

5.1 Free swimming sperm cell

The most common sperm cells are free swimming sperm cells with one flagellum. The flowfield of the free swimming sperm cell is depicted in figure 14. In the flow field it can be seen that the fluid is moving in the opposite direction of the movement of the sperm head. Additionally, it can be observed that the fluid is being propelled as usual.
The average velocity of the tail in the free swimming case is modelled and depicted in figure 15.

5.2 Static load case

Sperm cells that undergo a static loading try to swim in one direction but the movement of the sperm cell is hindered by a static load acting opposite to the moving direction. A static load may exist for a sperm cell of which its head is fixed to a surface. When this is true, the sperm cell can be modelled as if it is subjected to a static load additionally to the sperm cell having one constraint at its fixed point. In order to model its behaviour and compare to a case with a free swimmer and a time-periodic load, a non dimensional averaged flow field can be obtained using Matlab. Since the collinear bundle is of main interest in this research. The static load case will be modelled using the average wave variables and viscosity ($25\mu$of the collinear

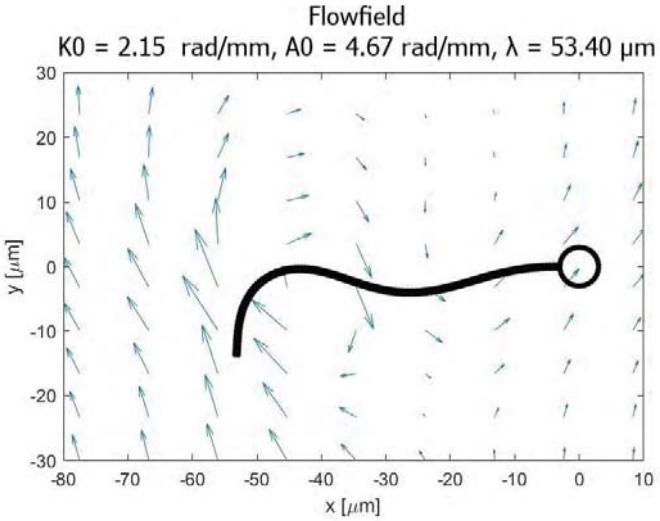

Fig. 14: Dimensionless velocity flow of the fluid around a free swimming sperm cell with one flagellum.

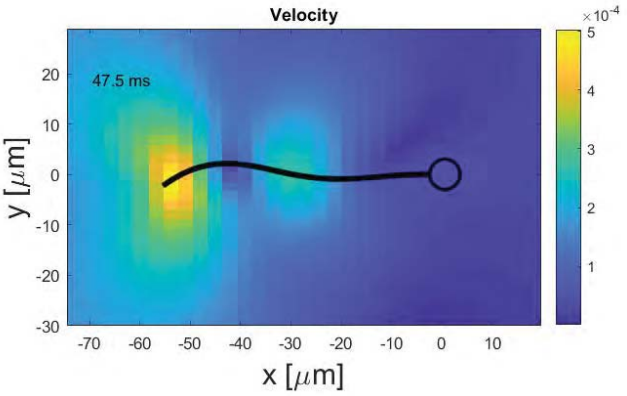

Fig. 15: Average velocity of the flagellum for a free swimming sperm cell with one flagellum.

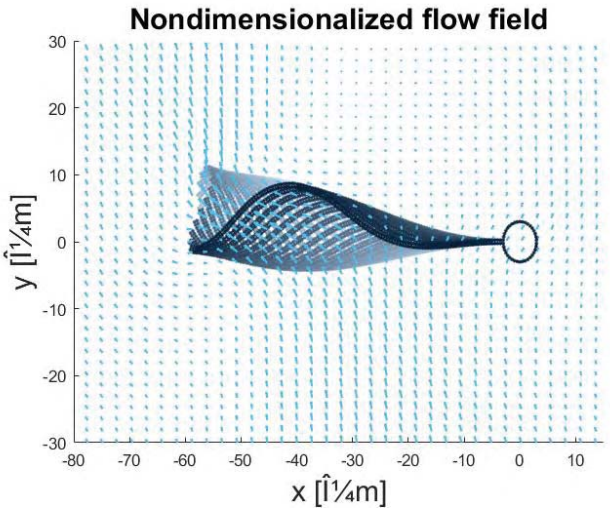

Fig. 16: Dimensionless velocity flow of the fluid around a static 1 tailed bundle.

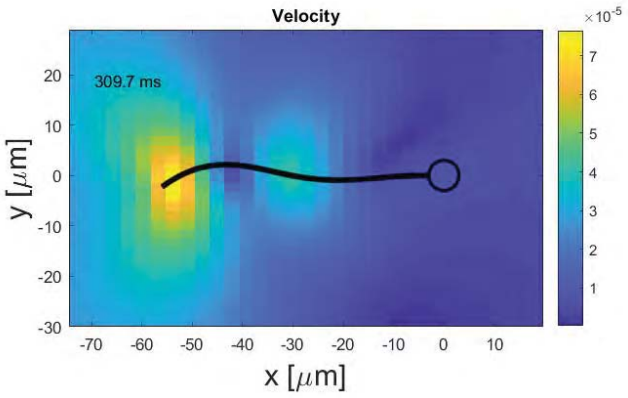

Fig. 17: Average velocity of the tail in static load case.

sample that was examined and are displayed in table 5.3. For this it is important to mention that the values of the left tail are used such that in the collinear case the left tail will be compared to the static and the free case. The left tail variables for the static case give the flowfield shown in figure 18 after one full beat cycle.

The average velocity of the tail in the static case is modelled and depicted in figure 17. It can be seen that the velocity is the highest at the end of the tail.

5.3 Time-periodic load case

When looking at a collinear bundle, one can see that while one tail tries to push the sperm cell forward, the second tail tries to push the sperm cell in opposite direction. From one tail its perspective this could be perceived as the second tail inducing a dynamic time periodic load on the sperm cell. The flow field of the sperm cell can be modelled in which the following averaged wave variables are used for each tail:

Tail:	$A_0(rad/mm)$	K_0 (rad/mm)	λ (μm)
Left Tail:	4.67	2.15	53.40
Right Tail:	3.76	1.76	86.74

Filling in these wave variables as input values in Matlab, a non dimensional flow field can be obtained. This flow field shows the velocity of the flow, in vector form, on average over multiple beat cycles and is depicted in figure 18.

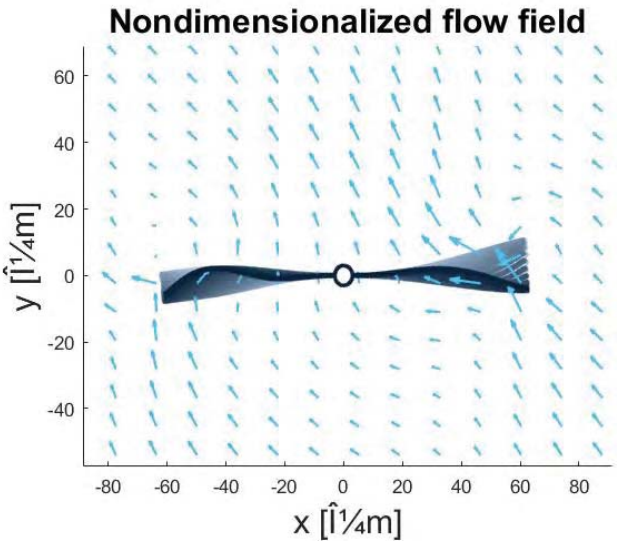

Fig. 18: Dimensionless velocity flow of the fluid around a collinear bundle.

Also the average velocities of the tails of the collinear bundle can be modelled and are shown in figure 19. Again it can be observed that the velocity is the highest at the point of the flagella furthest away from.

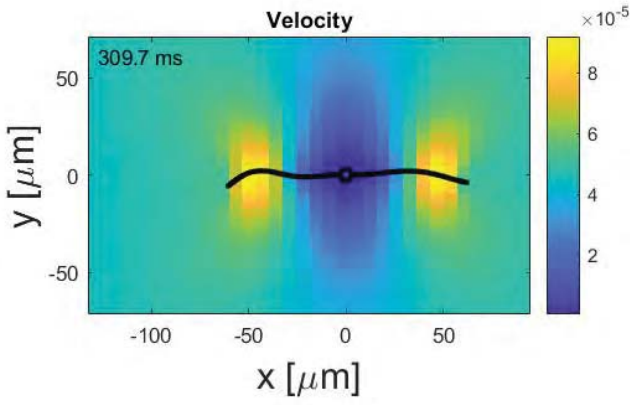

Fig. 19: Average velocity of the tails in a collinear bundle.

6 CONCLUSION

The close analogy between sperm cells and soft microrobots enables experiments to be conducted with sperm rather than building soft microrobots and experimenting with those. Sperm cells can be observed and wave variables governing the shape of the flagellum can be extracted for different sperm cell samples. A rare case of a sperm cell is a collinear bundle, which remains stable at $\delta\Theta(^\circ) = 180$. This is caused by a combination of steric and adhesive forces, for which holds that the adhesive force constant is larger than the steric force constant $\kappa_a > \kappa_c$. When increasing the value of $\frac{\kappa_a}{\kappa_c}$ the time between the initial collision of both sperm cells and when the collinear form is stable at $\delta\Theta(^\circ) = 180$ decreases (equilibrium is reached faster).

Wave variables are extracted for both flagella in the collinear bundle and a graph has been made showing how the wave variables change over time from a video which contains a collinear sperm bundle. From the wave variables it was concluded that large fluctuations in the assymetry parameter K_0 are a result of the disturbed oscillations of the head. These disturbances lead to high fluctuations in the head position. Therefore the value for the assymetry of the flagella changes a lot over time. Furthermore, the forward velocity v decreases substantially when the wavelength of both tails are equal $\lambda_{tail1} = \lambda_{tail2}$. Lastly, implementing resistive force theory on a collinear bundle can model the propulsion of the collinear bundle and it was shown that the thrust force of one flagellum is higher than the thrust force of the other flagellum. Regularized stokeslets theory has shown that the flowfield around a collinear bundle can be modelled and that the velocity of both flagellum increases with the distance away from the sperm cell its head.

ACKNOWLEDGEMENTS

I would like to thank I.S.M.Khalil for introducing me to the topic, giving very useful advise and tutoring me during this bachelorassignment. I learned a lot during this module about doing research to topics i knew little about from the start. Learning how to get familiar with the topic, looking what has already been researched and then looking at how I am able to contribute are all things I.S.M.Khalil has helped me with during the assignment. Furthermore I would like to thank Zihan Wang, who has been working on the same topic as me, collinear frames, during this research and has put in a lot of time and effort to assist me in my research. I would like to thank Jitse Leeftink for the good cooperation, giving me advice when needed and in general being a good working partner during this module.

REFERENCES

1. B. J. Nelson, Ioannis K. Kaliakatsos, and Jake J. Abbott, Microrobots for minimally invasive medicine, *Annual Review of Biomedical Engineering*, (2010), 12:55–85.
2. G. J. Hancock and Maxwell Herman Alexander New-man, The self-propulsion of microscopic organisms through liquids, *Proceedings of the Royal Society of London. Series A. Mathematical and Physical Sciences*, (1953), 217(1128):96–121.
3. I. S. M. Khalil, A. F. Tabak, Y. Hamed, M. E. Mitwally, M. Tawakol, A. Klingner, and M. Sitti, Swimming Back and Forth Using Planar Flagellar Propulsion at Low Reynolds Numbers, *Advanced Science*, (2018), 5(2):1–9.
4. I. S. M. Khalil, A. Klingner, and S. Misra, Mathematical modeling of swimming soft microrobots, Academic Press, pp. 125-138, (2021).
5. I. S. M. Khalil, A. Klingner, and S. Misra, Mathematical modeling of swimming soft microrobots, Academic Press, pp. 1-14, (2021).
6. D. J.G. Pearce, L. A. Hoogerbrugge, K. A. Hook, H. S. Fisher, and L. Giomi, Cellular geometry controls the efficiency of motile sperm aggregates, *Journal of the Royal Society Interface*, (2018), 15(148).
7. B. M. Friedrich, I. H. Riedel-Kruse, J. Howard, and F.Jülicher, High-precision tracking of sperm swimming fine structure provides strong test of resistive force theory, *Journal of Experimental Biology*, (2010), 213(8):1226–1234.
8. B. Y. J. Gray and G. J. Hancock, The Propulsion of Sea-Urchin Spermatozoa, *Journal of Experimental Biology*,(1955), 32(4):802–814.
9. R. Cortez, The method of regularized stokeslets, *SIAM Journal on Scientific Computing*, (2002), 23(4):1204–1225.
10. R. Cortez, L. Fauci, and A. Medovikov, The method of regularized Stokeslets in three dimensions: Analysis, validation, and application to helical swimming, *Physics of Fluids*, (2005), 17(3):1–15.